Direct Control of Bearingless Permanent Magnet Slice Motor Based on Novel Flux Linkage Observer

Zhuheng Zhao, Huangqiu Zhu, and Yizhou Hua

School of Electrical and Information Engineering, Jiangsu University, Zhenjiang 212013, Jiangsu, China
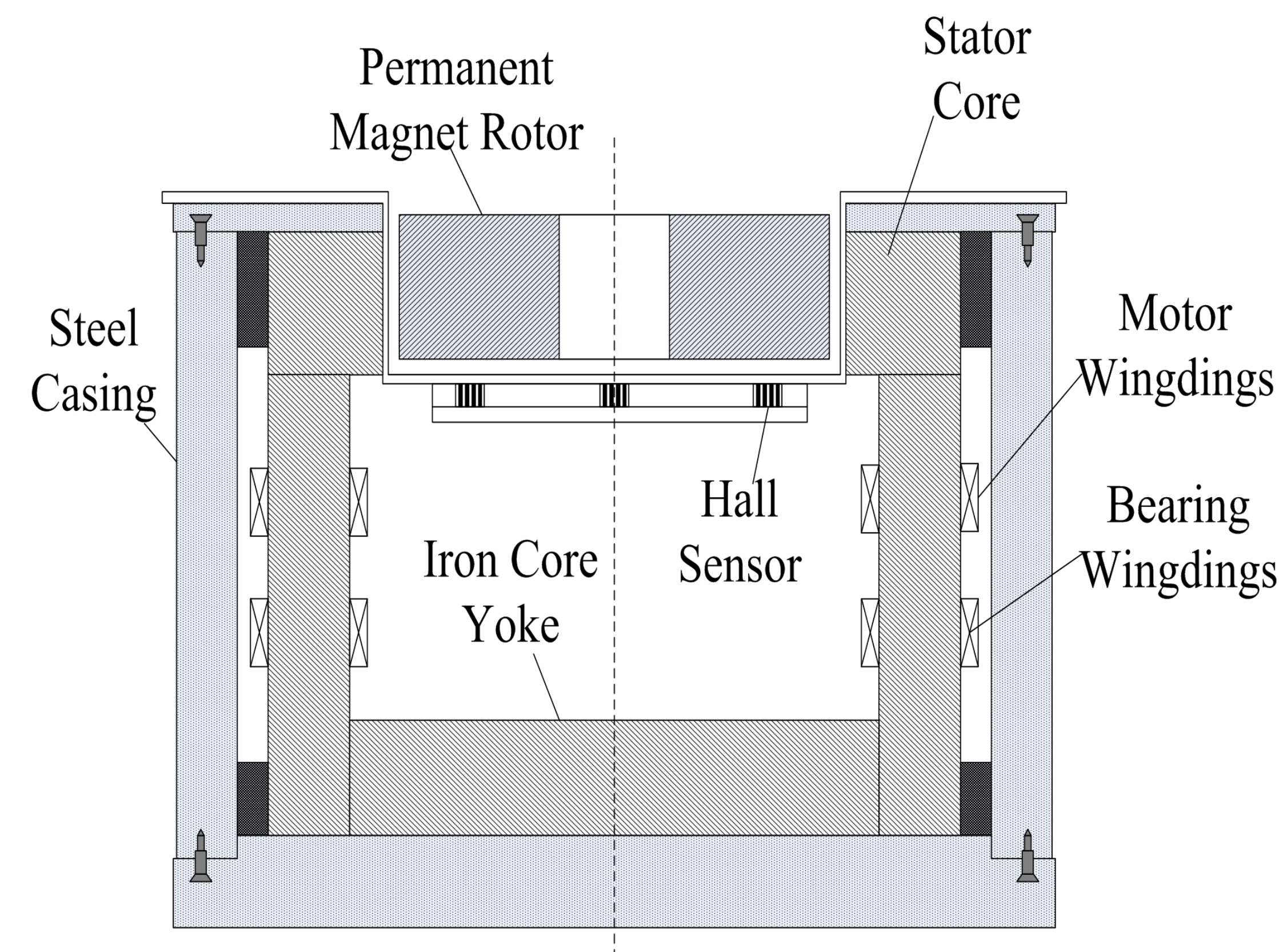
Background

A bearingless permanent magnet slice motor is a new research field of permanent magnet (PM) motor, which also inherits the merits of the magnetic bearing, such as no friction, no wear, no lubrication, long life, and so on. In addition, the unique feature of this motor is the passive stabilization on three degrees of freedom (one axial displacement and two tilting degrees of freedom) by the special rotor structure which axial length is quite shorter than the rotor diameter. Compared with other fully magnetically levitated systems, such system simplifies the mechanical structure and reduces the difficulty of control, which lead to an important research value and application potential prospects in the special electric drive fields, such as medical industry, semiconductor, and chemical industry.
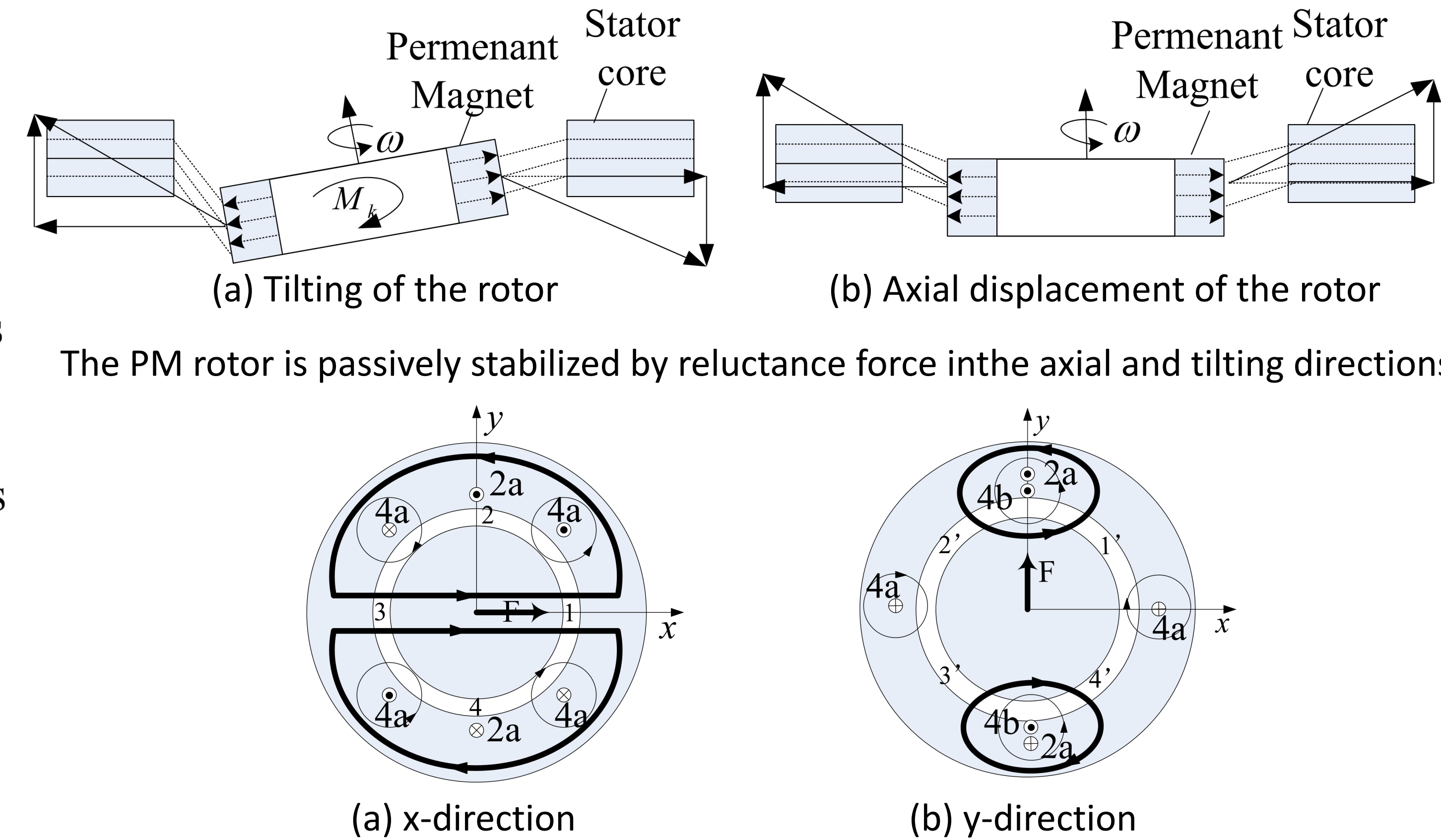
Objectives

❖ Designing flux observer and constructing prediction control model
❖ Testing control system by simulation and experiment

Basic structure and working principle of the BPMSM

(a) Tilting of the rotor   (b) Axial displacement of the rotor

The PM rotor is passively stabilized by reluctance force in the axial and tilting directions.

(a) x-direction   (b) y-direction

The stator of the motor is distributed evenly around the rotor with six L-shaped iron core legs. Each of the motor windings and bearing windings of the BPMSM, whose numbers of pole pairs are $P_M=1$ and $P_B=2$, respectively, has six concentrated coils distributed on the iron core leg.

As a function of the two magnetic fields with different numbers of pole pairs, the original balanced air-gap magnetic field is broken and in this case a radial suspension force can be generated to realize the rotor stabilization. As shown in (a), the flux density in air gap 1 is strengthened and by contrast, that in air gap 2 is weakened. Thus, a suspension force component F is generated in the x-direction.

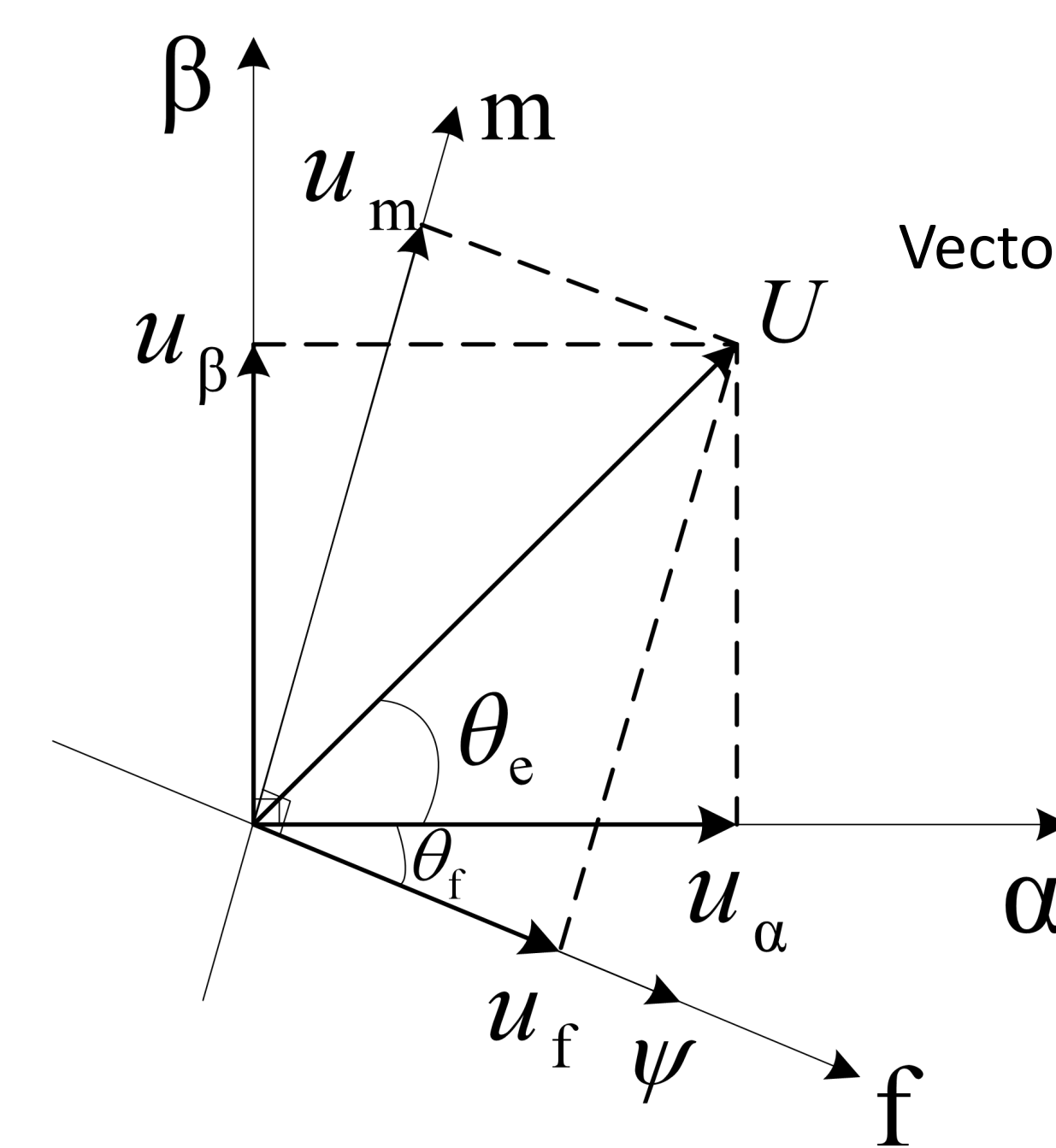## Flux Linkage Observer Based on Phase-Locked Loop

Flux linkage observer based on the PLL
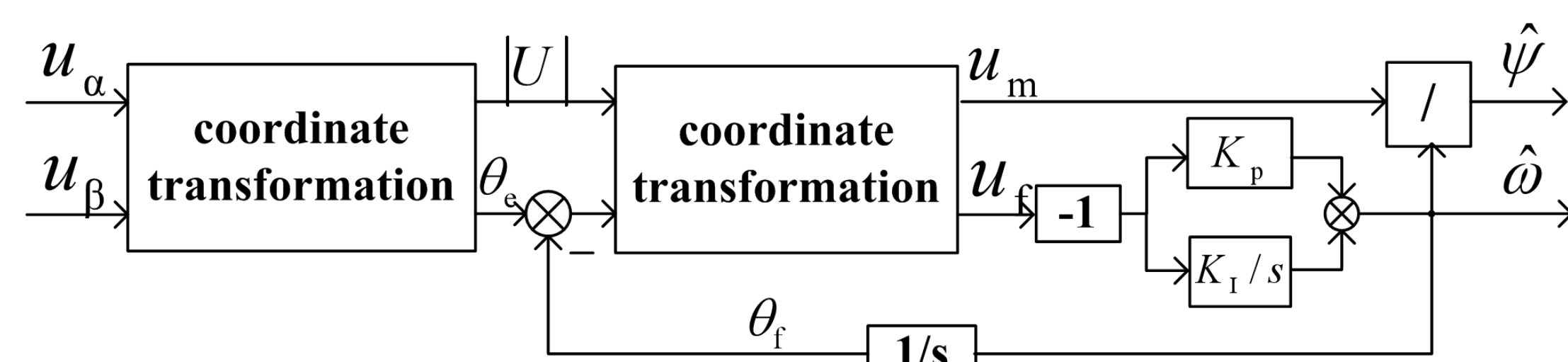
Closed-loop transfer function: $g(s) = \dfrac{K_P s + K_I}{s^2 + K_P s + K_I}$

The steady state output: $\begin{cases} \hat{\omega} = g(s)\theta_e \\ \hat{\psi} = u_m / \hat{\omega} \\ \theta_f = \int_0^t \hat{\omega}\,dt \end{cases}$

Vector diagram of flux linkage and voltage

Vector relation: $\begin{cases} |U| = \sqrt{u_\alpha^2 + u_\beta^2} \\ \theta_e = \arctan\left(u_\beta / u_\alpha\right) \end{cases}$

$\begin{cases} u_f = |U|\cos(\theta_e - \theta_f) \\ u_m = |U|\sin(\theta_e - \theta_f) \end{cases}$

Prediction Control Model

Electromagnetic torque

Torque observation:

$$T_e(k+1) = \frac{3}{2}\left[\psi_{s1\alpha}(k+1)i_{1\beta}(k+1) - \psi_{s1\beta}(k+1)i_{1\alpha}(k+1)\right]$$

Reference voltage calculation:

$$\begin{cases} u_{1\alpha}^* = R_{s1}i_{1\alpha}(k+1) + \dfrac{\psi_{s1}^*\cos(\lambda_1 + \Delta\delta) - \psi_{s1}\cos\lambda_1}{T} \\ u_{1\beta}^* = R_{s1}i_{1\beta}(k+1) + \dfrac{\psi_{s1}^*\sin(\lambda_1 + \Delta\delta) - \psi_{s1}\sin\lambda_1}{T} \end{cases}$$
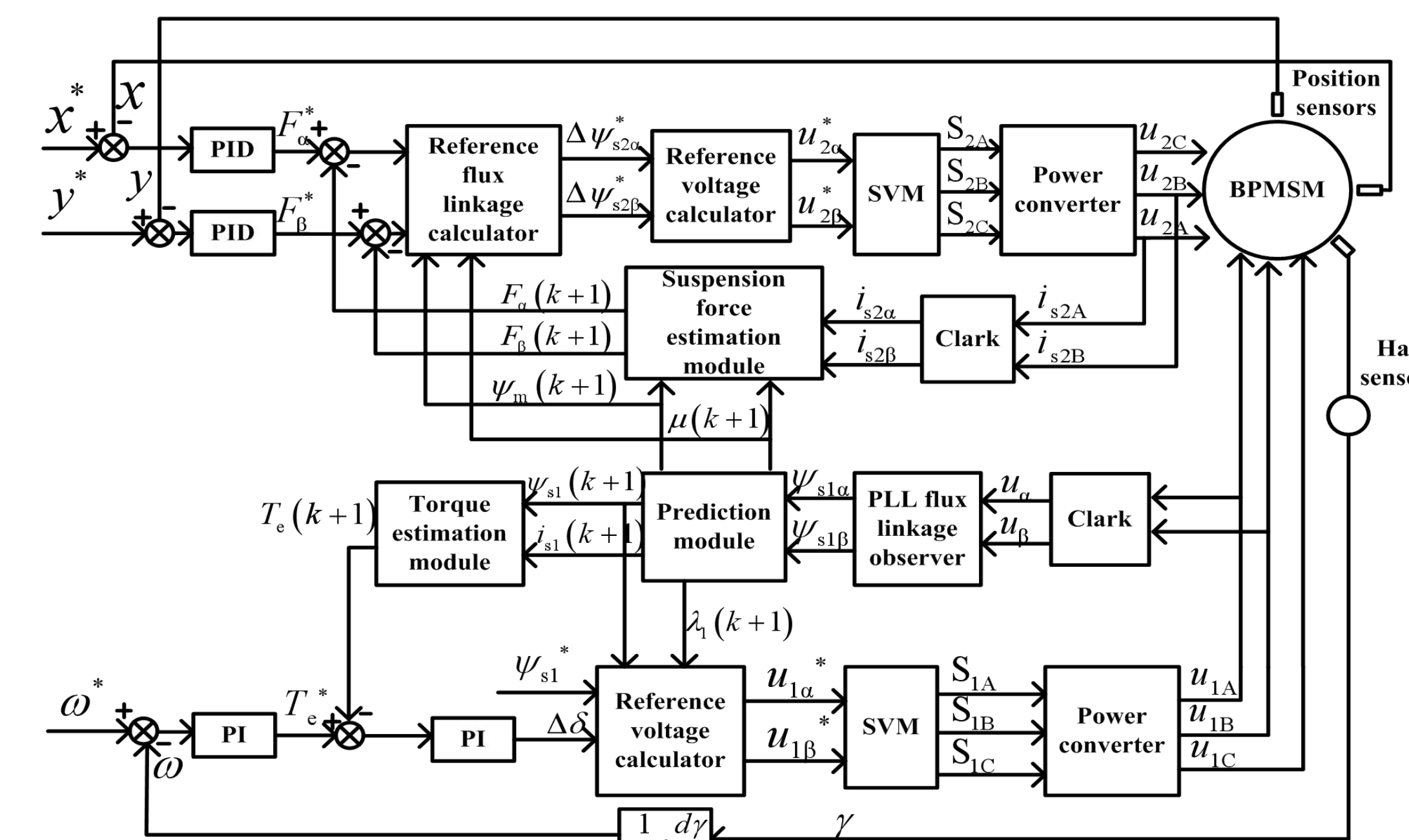
Suspension force

Suspension force observation:

$$\begin{cases} F_\alpha(k+1) = k_m L_{m2}\left(i_{2\alpha}\psi_{m\alpha}(k+1) + i_{2\beta}\psi_{m\beta}(k+1)\right) \\ F_\beta(k+1) = k_m L_{m2}\left(i_{2\beta}\psi_{m\alpha}(k+1) - i_{2\alpha}\psi_{m\beta}(k+1)\right) \end{cases}$$

Reference voltage calculation:

$$\begin{cases} u_{2\alpha}^* = R_{s2}i_{2\alpha} + k_M^{-1}\psi_m^{-1}(k+1)\left(\Delta F_\alpha\cos\mu + \Delta F_\beta\sin\mu\right) \\ u_{2\beta}^* = R_{s2}i_{2\beta} + k_M^{-1}\psi_m^{-1}(k+1)\left(\Delta F_\alpha\sin\mu - \Delta F_\beta\cos\mu\right) \end{cases}$$

Simulations

Direct control system of the BPMSM

Simulation results

As shown in (a)–(c), speed is set to 6000 rpm, speed overshoot is under 0.2%, and the fluctuating error of speed in steady state is less than 10rpm. Motor load torque is 0.5 N·m at starting, and then added to 3 N·m at 0.13 s. The pulsating movement of torque is less than 10%. Fig. 6(c) shows the tracking performance of torque windings flux linkage, the fluctuating error of the amplitude in steady state is very small. Fig. 6(d) shows the comparison results of the rotor radial displacement curves in the x-direction when two different flux linkage observation methods are used in direct control, respectively. The red solid line represents the method proposed in this paper. The blue dotted line is the rotor displacement curve derived from the traditional method based on the voltage-current model. A comparative analysis of experimental results is made between the proposed method and traditional method, as shown in Fig. 6(e) and Fig. 6(f).
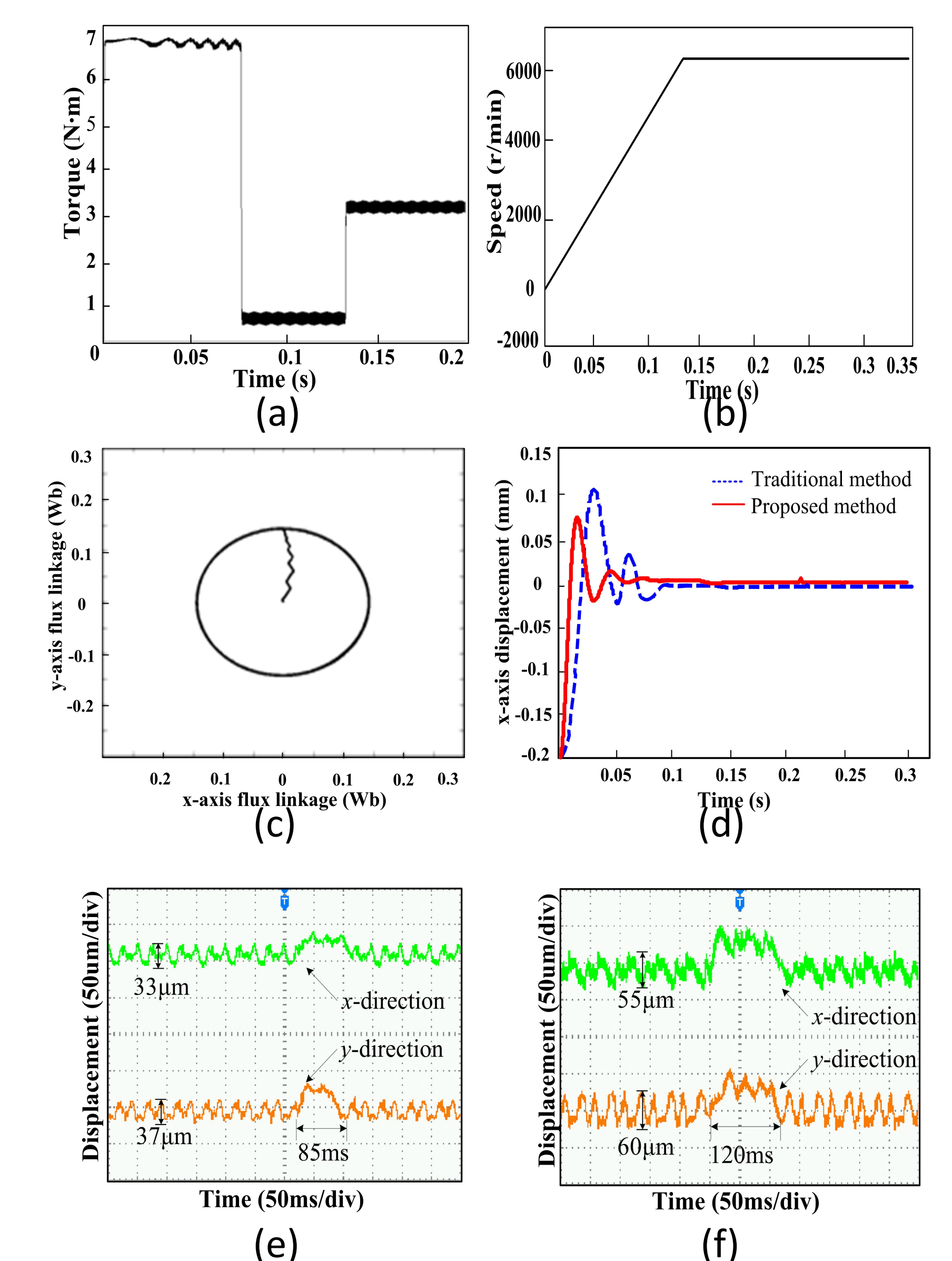
Conclusions

✓ According to the closed-loop transfer function, the response speed of flux linkage observer is only related to the observer coefficients and is independent of the rotor speed, which enhance the rubustness of the system.
✓ The observational lag is compensated by the prediction control module, which greatly increase the control accuracy and response speed of the suspension force.
✓ The decoupling control of the BPMSM is realized and a good anti-interference ability is achieved.